UT26 Design Binder

Vehicle Controls

09.07.2026

Mo Taban
Jaden Zhang
David Li
Hunzala Rajput

Contents

1. Brakes

Fundamentally, the brakes of an FSAE car stops the car by converting the kinetic energy of the car into heat. The brakes can be split into three sub-assemblies: the rotor and caliper assembly, brake lines and brake pedal. To actuate the brakes, the driver presses the brake pedal, pushing hydraulic fluid from the master cylinders, through the brake lines and into the pistons of calipers, which push brake pads into the brake rotors, creating friction and dissipating heat to stop the car. The following sections will detail the calculations needed to design a FSAE brakes system and the design of the UT26 brakes system.

1.1. Brake Design Fundamentals

A full, in-depth explanation for the brakes calculations is given in the UTFR Brakes Calculation Guide by Asal Ghorbani (UT23 Brakes Lead) and the full calculations can be found in the UT26 Brakes Calculation Sheet. In short, we design the brakes for maximum braking, meaning we design the brakes to provide the force for all four wheels to lock up at the same time. We estimate a maximum deceleration, calculate the weight transfer to the front axles (using the mass, front-rear mass distribution, wheelbase, and center of gravity of the car) and sum up the downforce on both axles, which gives us the normal force on each tire, and using the coefficient of friction of the tires, we can find the maximum friction force between the tires and the ground. Using this and the tire radius, we can calculate the maximum torque that can be applied to the tires, and using the effective caliper pad radius and coefficient of friction, we can find the caliper piston clamping force. Then, using the caliper piston diameter, we can calculate the brake fluid pressure in the front and rear lines. Next, using the master cylinder bore size we can calculate the required force on the front and rear master cylinders. Finally, we calculate the pedal mechanical advantage (effectively a level effect) and then can calculate the total force required on the brake pedal to achieve maximum braking.

1.2. Rotors

When designing our brake rotors, the biggest considerations are the sizing (which is limited both by calipers and wheel rim size), the strength, and the temperature the rotors will reach. To achieve the largest braking torque, the rotors are designed to have the largest radius possible while ensuring enough clearance between the caliper and wheel rim. To mount the rotors to the hub, bobbins are used, which allow the rotors to “float” relative to the hub instead of being rigidly connected. The material used for the rotors in the past has always been steel, specifically 1020 steel, as opposed to aluminum due to its higher strength. To enhance cooling and reduce the mass of the rotors, cross drilled holes and slots were added. This theoretically improves airflow and allows for debris to be cleared, although we have no concrete simulation or testing validation. A wave pattern around the edge was also added for a similar reason. From the previous principles, the brake rotors were designed and were not changed for many years. UT24 brake rotors are shown below as an example.

Figure 1: UT24 Brake Rotor

Many changes were made in the design of UT26 rotors. As part of our sponsorship with Brembo, we received feedback on our previous rotor design. The Brembo contact suggested simplifying the geometry, particularly removing the wave feature and using only slots or only holes, and spreading out the rotor mounting points evenly rather than 3 pairs. The rotor material was also changed to Hardox 450 Steel. Compared to 1020 Steel, it has a much stronger yield strength (1250 MPa vs 350 MPa) and hardness (450 HBW vs 121 HBW). This improves wear resistance and provides an even larger safety factor. The UT26 brake rotors are shown below.

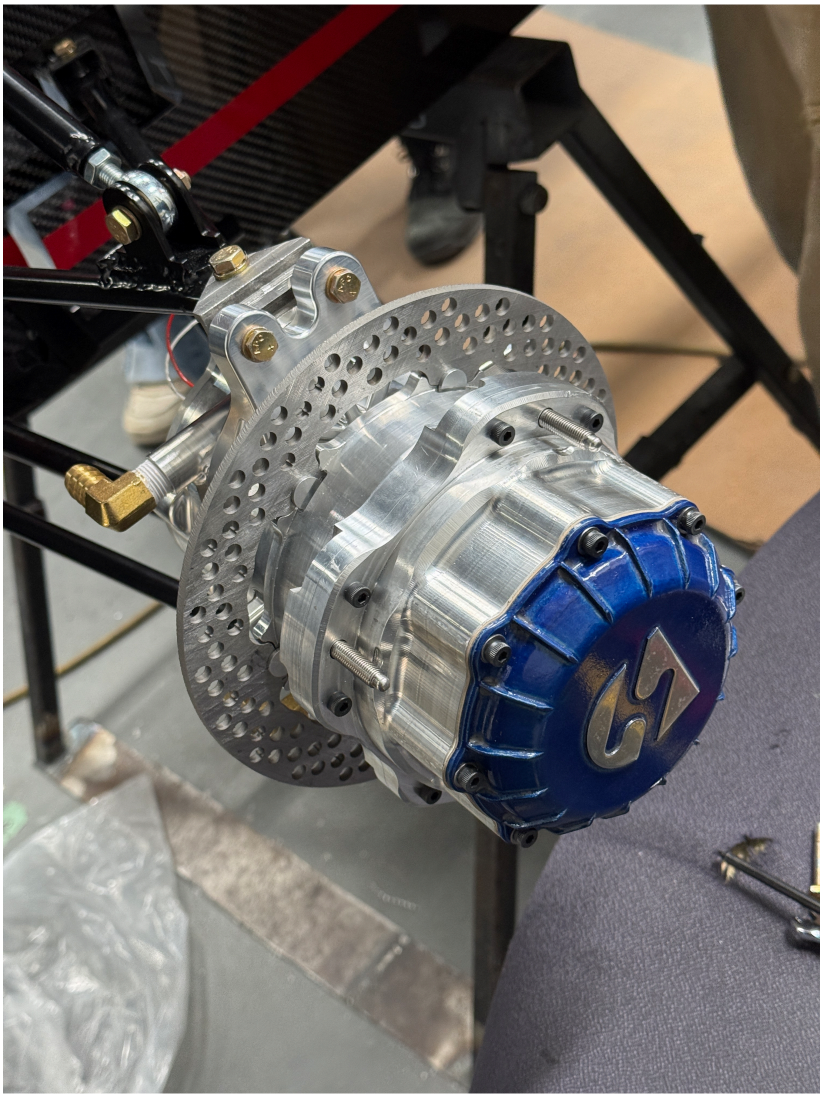

Figure 2: UT26 Brake Rotor

1.2.1. Heat Transfer Calculations

Notes:

- all units are SI unless stated otherwise
- braking acceleration is defined as negative
- its assumed that 95-98% of energy from braking goes into the rotor, 2-5% flows into pad, fluid

Before going any the formulas, we must first cover some concepts in heat transfer.

When modelling the heat transfer in the rotors, we are concerned with conduction, which is heat transfer from direct physical contact (pads and rotors, pads and caliper, within the rotor, caliper and pads) and convection, which is heat transfer through the physical movement of fluids. When the car is moving, the rotors are cooled via *forced convection*, where the physical movement of the fluid (air) is caused externally rather than due to buoyancy of the fluid. Heat transfer due to convection is directly proportional to both the area of heat transfer and the temperature difference:

$$\dot{Q} = hA\Delta T$$

h is the convection heat transfer coefficient with units of $W/m^2 \cdot K$.

We must also understand some basic fluid dynamics to understand convection. A fluid is a liquid, gas or other substance that continuously moves and deforms when a shear stress is applied to it, and cannot resist any shear force applied to it, unlike a solid, which can return to its original shape when the shear force is released. Viscosity is the property of a fluid that describes its resistance force when there is relative motion between it and another fluid body. An example of a more viscous fluid is glue, while a low viscosity fluid is water. Viscosity can be described as dynamic viscosity (μ), with units of $Pa \cdot s$. Dividing a fluid's dynamic viscosity by its density gives kinematic viscosity (ν), with units of (m^2/s).

Now, we can model the rotors as a lumped capacitance system, where heat is generated from friction between the pads and the rotors, and the heat is dissipated from the rotors via external forced convection. The lumped capacitance method assumes that the temperature within the system (rotors) does not vary across its dimensions, aka the temperature is uniform throughout. This assumption is valid as long as the conductive heat transfer with the system is large enough compared to the convective heat transfer, and this is characterized by the Biot number:

$$Bi = \frac{hL}{k}$$

L is the characteristic length (dependent on geometry, often calculated as the volume divided by heat transfer area) and k is the thermal conductivity. A Biot number of less than 0.1 generally means the lumped capacitance method is valid.

We will now describe how the heat generation and heat dissipation is calculated below.

Heat Generation Model

There are two ways of determining the heat generated during a braking event. Method one uses the kinetic energy of the vehicle and assumes that in a braking event, all of that kinetic energy is converted to thermal energy through the friction between the brake pad and the rotor.

$$E_k = \frac{1}{2}m(v_2^2 - v_1^2)$$

From this, in order to determine the energy in watts, simply divide the E_k by the duration of the braking event.

$$\dot{Q} = \frac{v_2 - v_1}{a}$$

The second method involves calculating the instantaneous power generated per wheel during braking. This method relies on the fact that power is calculated as torque multiped by angular velocity, which are both know variables for the rotors.

$$\dot{Q} = T\omega = \mu_{\text{pad}} F_{\text{clamp}} r_{\text{effective}} \omega$$

Heat Dissipation Model

The method for determining the heat dissipation during a braking event is slightly more complex and requires some assumptions to be made. The best we can do is approximate the rotor as a simpler geometry and calculate the convection heat transfer coefficient with some empirical relationships.

A few important quantities are needed to find the convection heat transfer coefficient.One of them is the Reynold's number. It can be calculated with the equation:

$$Re = \frac{\rho v L}{\mu}$$

ρ is the fluid's density, v is the fluid speed and L is the characteristic length, dependent on if its internal or external flow, and the geometry the fluid is flowing around or through (eg. the diameter of a pipe). A lower Reynold's number is indicative of smooth, laminar flow, whereas a higher Reynold's number is indicative of chaotic, turbulent flow. The specific numbers defining laminar and turbulent flow differs between internal and external flow.

Another important dimensionless number is the Prandtl number. It describes the ratio between a fluid's momentum diffusivity and thermal diffusivity and is calculated as:

$$Pr = \frac{\nu}{\alpha}$$

The last important number we will need is the Nusselt number. It represents the ratio between convective and conductive heat transfer across a boundary and is calculated as:

$$Nu = \frac{hL}{k}$$

Although this equation looks identical the Biot number equation, the key difference is that the thermal conductivity k is for the fluid.

We can now calculate the heat transfer coefficient by using the empirical relation for the average Nusselt number for turbulent flow over a flat plate.

$$\overline{\mathrm{Nu}}_L = 0.037 Re_L^{0.8} Pr^{\frac{1}{3}}$$

Rearranging the Nusselt equation from earlier, we can solve for the convective heat transfer coefficient.

$$h = \frac{\overline{\mathrm{Nu}}_L k}{L}$$

$$\dot{Q} = hA\Delta T$$

1.2.2. Determining Temperature

To calculate how the temperature changes, we need to know the specific heat of the rotors, c_p, which describes the amount of energy required to raise a unit mass of a material by 1 K, and has units $(J/kg \cdot K)$. The heat needed to increase the temperature of the rotor of mass m over a period of time t is:

$$\dot{Q} = \frac{mc_p \Delta T}{t}$$

Considering both the heat generation from braking and heat dissipation from convection, we can then calculate the change in temperature of the rotor:

$$\Delta T = \left(\frac{\dot{Q}_{\text{conduction}} - \dot{Q}_{\text{convection}}}{mc_p} \right) t$$

1.3. Proportioning Valve

As mentioned before, the brakes are designed to perform under maximum deceleration. However, when the car is experiencing deceleration less than maximum, less weight will transfer to the front and the front will lock before the rear. Therefore, we need a method to adjust brake balance. The first of these is the balance bar. By adjusting the balance bar clevice position, the proportion of force applied on each master cylinder push rod can be adjusted.

Figure 3: UT26 Balance Bar

However, the balance bar cannot be used with a driver in the car and while the car is driving. This is where the proportioning valve comes in. The proportioning valve connects the rear master cylinder to the rear brake line circuit. By adjusting the proportioning valve position, the pressuring going into the rear brake circuit can be reduced. The pressure curve for the proportioning valve used for UT26 is shown below:

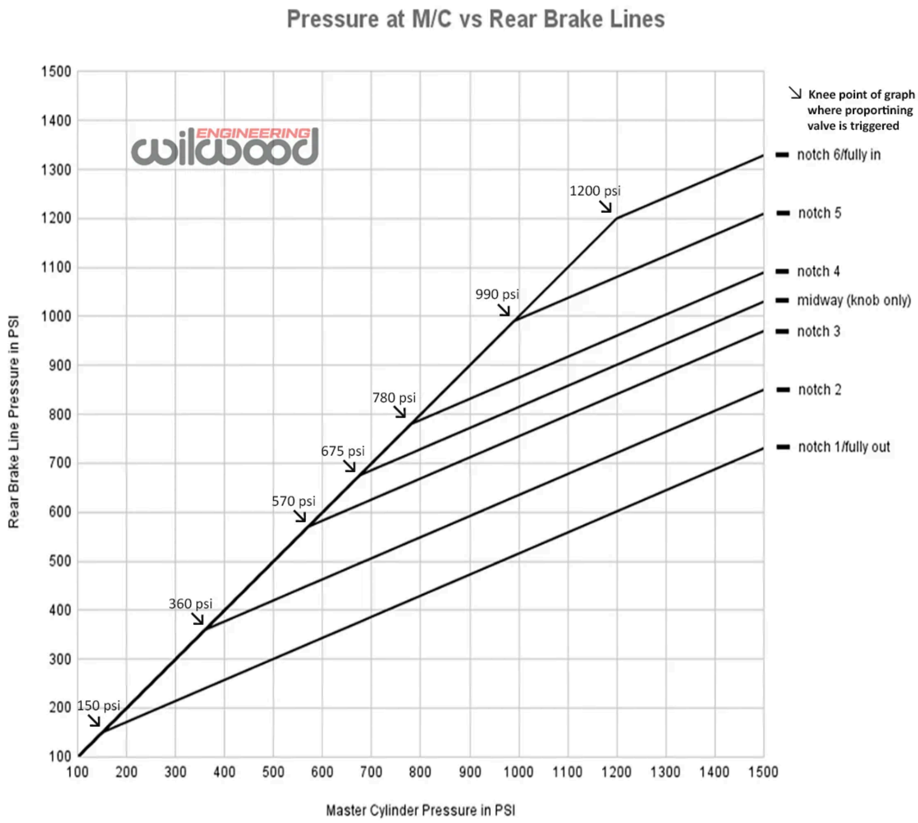

Figure 4: Proportioning Valve Pressure Curve

More in depth information about the proportioning valve can be found in the UT26 Proportioning Valve Documentation by Jaden Zhang.

1.4. EBS

As a key component of the driverless/autonomous system at the Formula SAE Electric and in European competitions, the Emergency Brake System, or EBS as it will be henceforth referred to, is the actuation system that engages the brakes and stop the car without driver input.

The system exists as a failsafe, being able to perform an Emergency Brake Maneuver at any point during Driverless dynamic events. At competition, this subsystem aims to pass EBS Test. At Formula SAE Electric EBS Test requires the driverless car to stop autonomously, after a period of straight line acceleration to 40km/h, within 8.5m, using the EBS System.

Additionally, this system is designed around the regulations specified in the Formula SAE Rules 2026, and the Formula SAE Driverless Supplement 2026, both of which can be found on their website. Some key rules are highlighted below.

- DT.3.2.1.a - The EBS must only use passive systems with mechanical energy storage.
- DT.3.2.5.a - The time between opening of the Shutdown Circuit and the start of deceleration must be 200 ms or less
- DT.3.2.5.b - In case of a single failure the EBS should achieve at least half of the performance.
- DT.3.2.5.c - The average deceleration must be more than 10 m/s^2 under dry track conditions.

Since we have a pneumatic (operated with compressed air) EBS system, some other key regulations are also applicable.

- T.6.1.2 The gas cylinder/tank must be commercially manufactured, designed and built for the pressure being used, certified by an accredited laboratory, and labeled or stamped
- T.6.1.3 The pressure regulator must be mounted directly onto the gas cylinder/tank
- T.6.1.5 - The gas cylinder/tank must be insulated from heat sources (including Radiation, Convection, Conduction)
- T.6.1.7 - The gas cylinder/tank must be securely mounted inside the Chassis, outside the Cockpit, below the Shoulder Belt Mount, and aligned so the axis does not point at the driver

The UT26 EBS changes the UT25 1-source + 2-storage tank design to a 2-source tank circuit design, keeping legality while simplifying components.

1.4.1. Pneumatic System Overview

The entirety of the EBS system, including the Mechanical Assembly Drawings and the Pressure System Overview are deliverables for the DSF submission.

The UT26 EBS system operates by have two independent pneumatic circuits for the front and rear brakes. Compressed air is stored in black airsoft tanks right behind the firewall, flowing to a normally-open solenoid and reaching an EBS piston assembly on the brake pedal tray to push down the master cylinder pistons, activating the hydraulic brakes as a driver would.

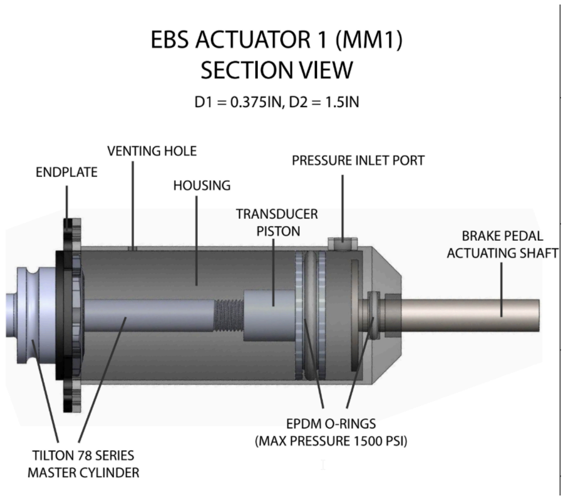

Figure 5: EBS Cylinder cross section. Left to MC; Right to pedal balance bar. From Pressure System Overview.

The specific pneumatic circuit can be found in the Pressure System Overview. For future reference of the UT26 main system, below is a labelled breakdown of the majority of the EBS circuit, up to connecting the actuating solenoids.

Figure 6: EBS storage tank and connected pneumatic components. Stored behind firewall.

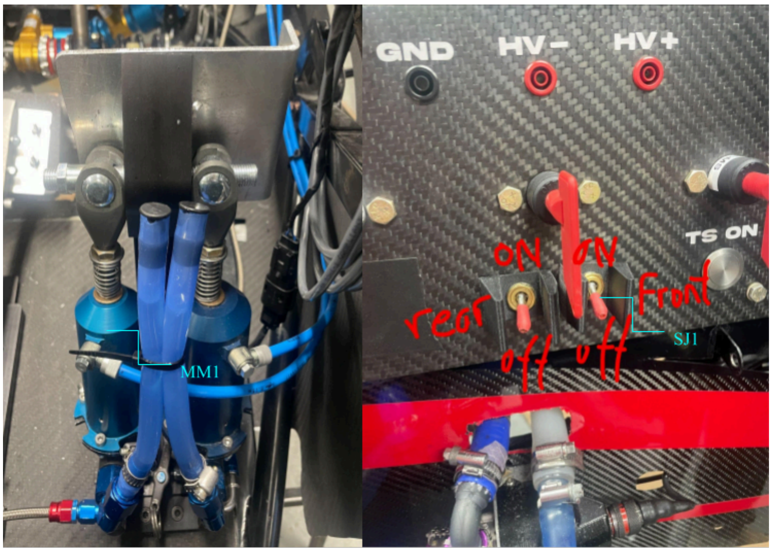

Figure 7: EBS Cylinnders and Manual Releases.

It should be noted that UT26 used CNC manufacturing for the (blue) cylinders. This was done to address leaking and tolerance issues from UT25 manual manufacturing methods.

Additionally, the EBS storage tank was moved to behind the firewall to allow for mounted refilling rather than requiring removal to refill. This is also partially due to the design focus of allowing the accumulator to be removed from the rear of the vehicle.

1.4.2. Key Calculations

The major calculations governing the EBS system are in this spreadsheet.

Generally, calculations for the EBS system dictate part selection and gauge pressure of the storage tanks. The spreadsheet does a thorough job of outlining the relevant variables in this system, so specific equations will not be explained here.

It should be noted that the UT26 calculations also puts into consideration the "dead" volume of air existing in the EBS tubing. This extra little volume does not impact the current system significantly, but a more tightly budgeted one benefits from the precision this calcuation adds.

Of course, this system has encountered a few difficulties.

- System assembly was difficult - The mounting of the EBS tanks and their mounts was almost completely physically blocked by the accumulator. This presented easily solvable issues in assembly order for these mounting pieces.
- Source tanks did not have real spec sheets - Sourcing airsoft components provided a large array of viable products, but also opened the door to documen-

tation issues. The tanks used in the UT26 system, Tippmann - 13ci, did not have proper online documentation, making data sheet submission more sketchy than it needed to be. Additionally, these tanks would require hydrostatic testing these years anyway, so it will likely be replaced.

2. Steering

Fundamentally, the steering system of any FSAE car works to change the heading of the vehicle by allowing the driver to control the front tires' angles, thereby generating lateral forces due to the slip angle, allowing the car to corner. The mechanical system connecting the driver to the tires can be viewed as two primary subsystems - the steering column, and the steering rack. As of the UT26 team structure, the steering wheel is Driver Interface's project, and anything past the tie rods are Suspension/Drivetrain.

2.1. Steering Design Fundamentals

When designing the overall steering system, a thorough understanding of steering fundamentals is essential, as these parameters dictate the vehicle's cornering behavior, stability, and overall tire performance.

While a solid grip of these principles is crucial, it should be emphasized that the overarching steering kinematic points and performance is decided in collaboration with the Vehicle Dynamics (VD) subsection. The VD team optimizes the vehicle's kinematics to best mesh with the desired performance of the car, and thus, the ideal steering geometry is often a blend of the VD team's optimal points and the physical constraints of the current vehicle.

Thus, the primary design challenge for a member working on the steering subsystem should not be to define the steering geometry from scratch, but rather to physically package the subsystems to best match the desired points and with minimal play/looseness, while also understanding the core principles that steering geometry revolves around.

2.1.1. Grip

At a fundamental physics level, grip is defined by the friction equation $F = \mu N$, where maximum grip (F) is determined by the coefficient of friction (μ), and the vertical load (N) pushing down on the tire.

A tire can only exert a force on the ground, whether that be longitudinal (acceleration, braking) or lateral (turning), it must have sufficient grip to keep it from simply sliding.

Higher grip naturally results from changing one of the two elements of the friction equation.

- Changing μ: A softer, stickier tire compound, ran at their optimal temperature, or improve the suspension geometry so the maximum amount of the tire's "contact patch" stays flat against the road can increase this coefficient. Think of many drag tires.

- Changing N: A higher vertical load increases the grip of the tire. Naturally, a heavier vehicle accelerates slower, and so this path of increasing grip is generally relevant to load transfer situations, such as longitudinal load transfer onto the front axle during braking, or lateral load transfer onto the outer wheels during a turn.

2.1.2. Slip Angle

A tire rolling perfectly parallel to the chassis generates no turning force. To produce the lateral force necessary to alter the vehicle's yaw, the tire's heading must deviate from its actual trajectory. This angular deviation is defined as the slip angle.

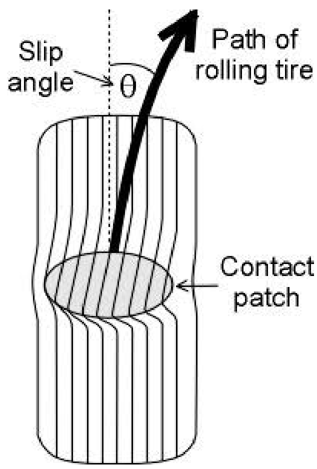

Figure 8: Tire slip angle and contact patch geometry.

When the driver turns the steering wheel, the steering rack pushes its tie rods to pivot the front uprights, introducing a slip angle. The friction between the track surface and the rubber causes the tire's contact patch to twist and elastically deform. This deformation generates the lateral force required to pull the front of the chassis into a turn.

2.1.3. Understeer/Oversteer

As mentioned in Asal's Brakes Calculation Guide (refer to 1.1), maximum frictional forces occurs right before sliding/skidding (dynamic friction) begins. Similarly for steering and tire grip, maximal steering grip is achieved when the slip angle of a tire is not so great that it begins sliding (but is close). Tuning the factors that lead to this is often the VD team's prerogative.

However, since braking and lateral forces on the front and rear axles are often purposefully unequal, a singular set of wheels can start to lock/slide before the other. A loss of grip in a corner by the front tires causes understeer, and the a loss of grip by the rear tires causes oversteer.

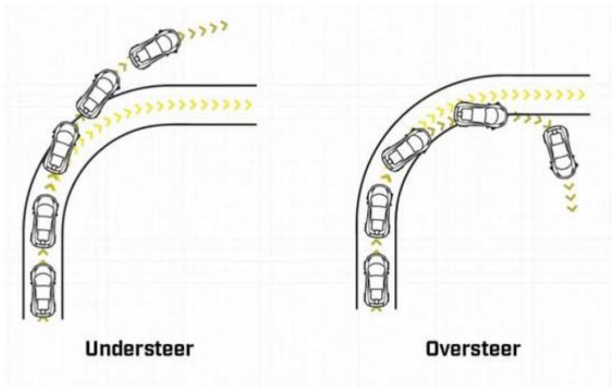

Figure 9: Understeer and oversteer visualization.

2.1.4. Camber

Similar to longitudinal acceleration, load transfer also occurs when lateral acceleration occurs. When cornering, the vehicle will experience roll in the direction opposite the direction of turning, which also impacts the roll of the tires. This, in turn, impacts the area of the contact patch, and thus grip. A perfectly vertical tire when rolling upright will lean slightly on one of its edges during a turn, reducing contact patch area, and therefore lowering grip.

Therefore, dynamic (moving) camber is typically designed to be negative, allowing the vehicle to roll onto its outside tires' flat face during a turn, maximizing grip there. Note that static camber is usually designated by the Suspension team's decisions.

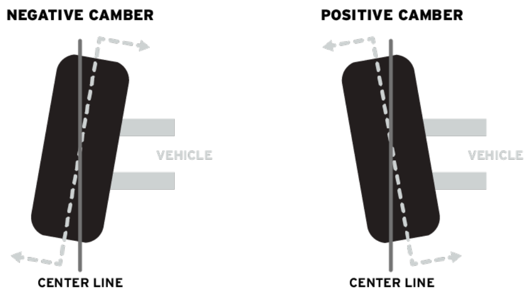

Figure 10: Camber visualization and sign convention.

Note that the outside tire's contact patch is 'prioritized' due to the lateral load transfer.

2.1.5. Ackermann Geometry

A core concept concerning the steering geometry as a whole is its Ackermann Geometry. When a car corners, because of its track, the outside tire will experience a circular path with greater radius than the inside tire, which is behavior that should be taken into account.

Ackermann steering geometry follows these travel lines, angling the inside tire more aggressively to allow all tires to more closely guide the vehicle. This geometry is generally more effective for lower speeds, but at higher speeds, sometimes provides insufficient lateral forces. Therefore, a common alternative is anti-Ackermann steering geometry, angling outside tires more aggressively to allow the heavily loaded (and thus higher grip) tire to reach its maximum lateral force.

UT26 runs a -10^o Ackermann geometry.

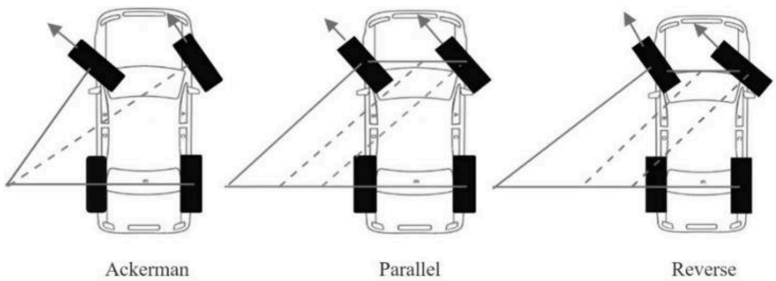

Figure 11: Ackermann and anti-ackermann steering.

2.2. Steering Column

Fundamentally, the steering column acts as the mechanical bridge between the driver and the steering rack. Its primary purpose is to transmit rotational torque and angular inputs from the steering wheel directly to the pinion gear inside the steering rack. Beyond angular transmission, the column must also rigidly support the steering wheel against driver inputs, while fitting within the chassis' ergonomic and structural boundaries.

The UT26 steering system features a two-column setup. The steering wheel is attached to the level input column with a quick disconnect (QD), which feeds into a double universal joint (U-joint) assembly, which redirects the rotational axis down to the secondary, output column. The secondary column terminates at the steering pinion gear, connecting to it with a spline coupler.

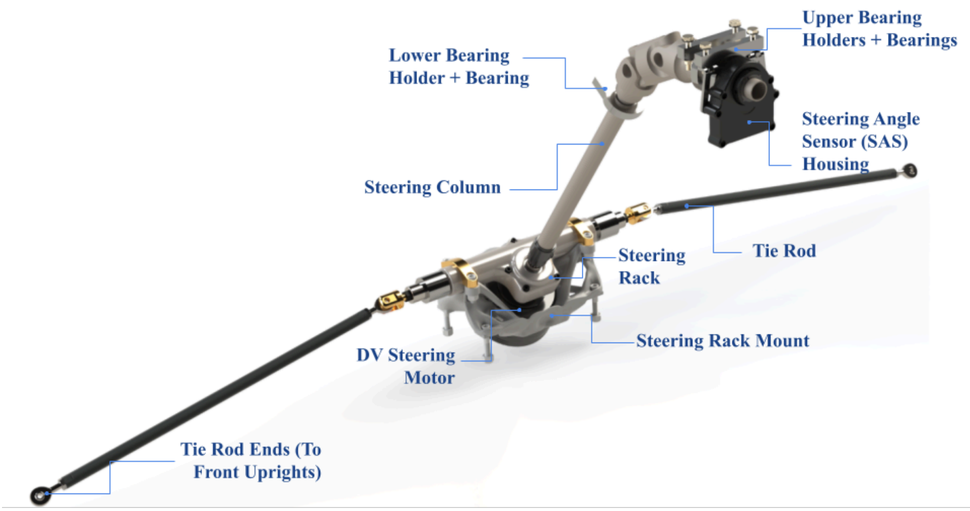

Figure 12: UT26 Steering system setup.

This system prioritizes packaging simplicity while also reaping the ergonomic benefits of flexible mounting positions. A single shaft setup (run by ETS, McMaster, etc) can present ergonomic and safety issues, while a three shaft setup (such as UT25's) is more difficult to engineer, especially requiring some precision in assembly.

2.2.1. The Universal Joint

A universal joint, or Cardan joint, is a mechanical linkage designed to transmit rotational motion between two intersecting, non-collinear shafts. The assembly consists of a central cruciform member (the cross or spider) connecting two perpendicular yokes attached to the respective shafts.

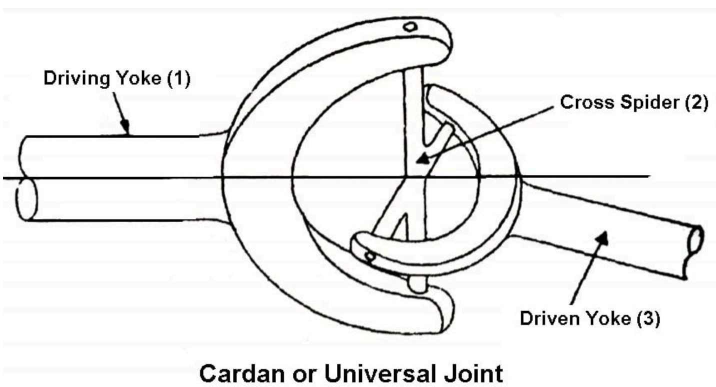

Figure 13: Cardan/universal Joint Geometry.

While effective for angular torque transmission, a single Cardan joint introduces a fundamental kinematic non-linearity into the system. When the input shaft is driven at a constant angular velocity, the output shaft does not rotate at a constant speed. Instead, it experiences a cyclic fluctuation, accelerating and decelerating twice per full revolution.

The magnitude of this velocity fluctuation is dictated by the operating angle (θ) between the two shafts; as the operating angle increases, the amplitude of the rotational error increases proportionally.

Within the context of aiming for a consistent and tight steering system, this non-linearity is a critical flaw. Implementing a single angled U-joint would induce a variable steering ratio dependent on the steering wheel's position, which would also scale based on θ. This would transmit a fluctuating, pulsing torque back through the steering column, effectively masking the tire's feel (akin to its pneumatic trail) and the lateral forces generated by the front tires, and compromising the driver's ability to accurately manage slip angles.

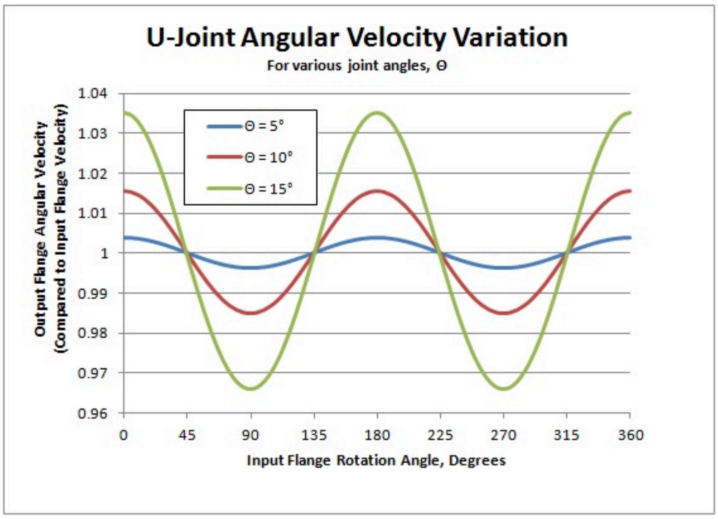

Figure 14: The output velocity variations of a singular u-joint.

To mitigate the kinematic errors inherent to a single Cardan joint and maintain a linear steering response, the UT26 steering architecture specifies an integrated double U-joint. Unlike a custom-fabricated intermediate shaft with two separate joints (which is commonly referred to as three-shaft system), this single component couples two Cardan joints within a combined central housing.

For any double U-joint system to function as a constant velocity joint, ensuring the final output shaft rotates synchronously with the initial input shaft, the cyclic acceleration of the first joint must be perfectly cancelled out by the cyclic deceleration of the second joint. Achieving this phase-cancellation relies on two strict geometric constraints:

- Correct Phasing: The internal yokes connecting the two joints must be perfectly coplanar. By utilizing a pre-manufactured double U-joint, this internal phasing is inherently fixed by the supplier, simplifying assembly.
- Equal Operating Angles: The operating angle between the primary column and the double U-joint assembly (θ_1) must be exactly equal to the operating angle between the double U-joint assembly and the secondary column (θ_2).

Figure 15: UT26 Double U-joint

With UT25's three shaft design, aligning two individual u-joints was a critical task that was phased out with UT26's design.

As such, the UT26 double u-joint was positioned such that its input and output angles were the same, though some manufacturing challenges required a slight pivot in orientation. This approach still retains the 1:1 linearity of having two u-joints, while simplifying packaging and assembly, requiring only two shafts, at the cost of a slight lowering in positional flexibility, making it a bit more difficult for the Driver Interface and Vehicle Dynamics teams to achieve their optimal steering wheel angle and steering rack angle.

2.2.2. Column Mounting

The UT26 steering column, as with all past years, is mounted with three ball bearings + bearing holders, bolted onto a steel mounting plate welded to chassis tubes, specifically to the front hoop. This structure provides support to ensure the steering column is sufficiently rigid when in operation under significant loads by the driver.

Figure 16: UT26 Steering column mounting plates/tubes

For UT26, the steering column loads were calculated using the max weightlifting forces by the 95th percentile male, providing a baseline for what the column tubes and its mounts must be capable of supporting. A more detailed report for these loads can be found in the UT26 Steering Calculations report by Noah Coles & Veronica Abdel Malak.

While useful, one of the points of improvement is to, in collaboration with UT27 Driver Interface team, gauge the true loads on the steering column using an adjustable steering rig.

It should also be noted that since the column mount is often welded to the chassis, and therefore is considered part of the chassis body, it essentially must be decided in position quite early in the season.

Another consideration for UT26 was sharing the space of the mounting plate/tubes with an advanced dash setup, somewhat limiting the usable space for effectively mounting.

2.3. Steering Rack

The steering rack is the mechanical assembly responsible for converting the rotational motion of the steering column into the lateral linear displacement required to pivot the front wheels. Operating via a traditional rack-and-pinion mechanism, the rotational torque applied by the driver (or the autonomous DV system) spins the pinion gear, which meshes with the straight rack gear to drive it left or right. This linear travel pushes or pulls the tie rods, which connect to the front wheel uprights, ultimately dictating the steering angle of the front tires.

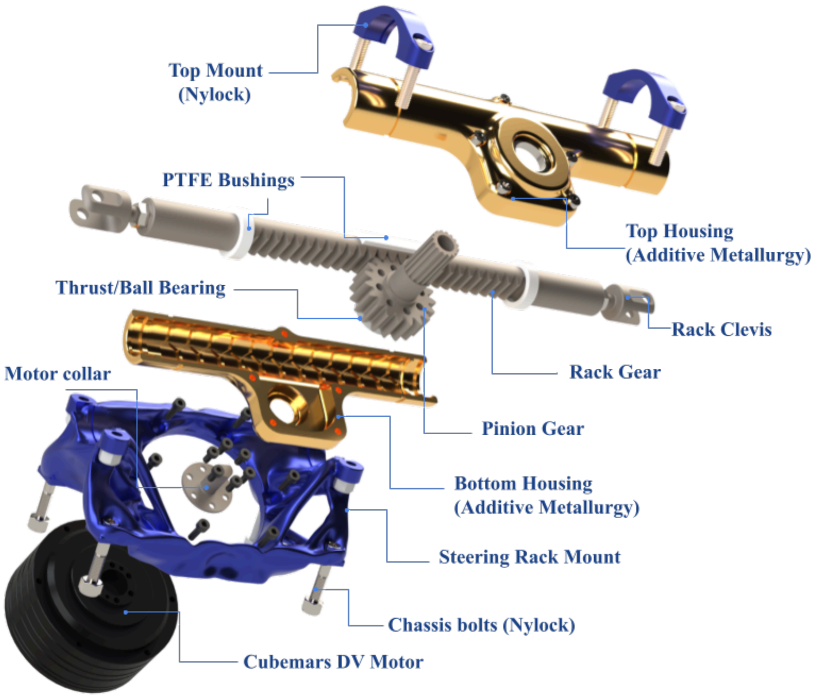

Figure 17: UT26 Steering Rack and SBW Assembly

A quick note on terminology - the entire assembly of the two gears, housing, bearings, etc, is referred to as the Steering Rack, while the actual linear gear is referred to as the Rack Gear.

The design parameters that went into constructing a safe and relatively inexpensive rack was done by Hunzala Rajput, with build data present for UT26 and the first iteration UT25, with extensive usage of the gearbox design software KISSsoft.

The UT26 steering rack featured an additively manufactured (AlSi10) housing, providing mass savings through cutout internal patterns. Additionally, the rack gear was slightly shortened to avoid interfering with the chassis/bodywork structure.

However, a prevalent problem in UT26 was the rack warping, bulging the middle of the rack towards the teeth, becoming a *banana*, after heat treating, an issue that persisted through multiple suppliers. The currently understood reason is that thorough heat treatment was done, while the rack gear only truly required case hardening (59HRC). This resulted in the rack gear catching on its PTFE bushings sometimes when moving through the steering rack.

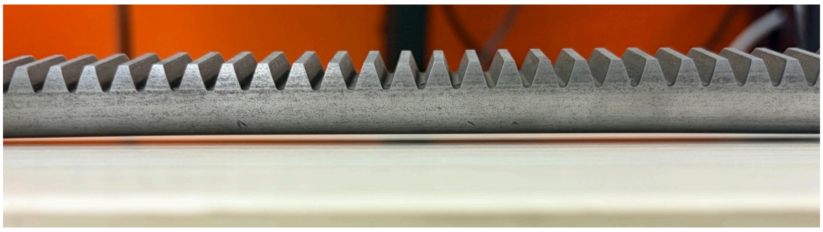

Figure 18: The slight warp towards the middle of the rack is barely visible, but significant in hindering performance.

As mentioned, the team utilized a fully custom-designed steering rack assembly. This continues a major architectural shift initiated during the UT25 season, definitively moving away from commercial off-the-shelf (COTS) units such as the Kazrack or Stiletto. The transition to an in-house design was driven by two primary engineering requirements:

Since UT25, the team has utilized a fully custom-design steering rack assembly. This initiative to move away from off-the-shelf units, such as the Kazrack or Stiletto Rack, to an in-house design was driven by two primary objectives:

- Geometric and Packaging Optimization: Commercial steering racks impose rigid constraints on tie-rod pickup points (clevis locations), physical footprint, and chassis mounting configurations. Designing a custom housing and rack shaft allowed the team to much more easily hit the exact kinematic hardpoints dictated by the Vehicle Dynamics team. Furthermore, it permitted a more optimized spatial envelope, allowing the rack to be packaged tightly against whichever external structure it was required to.

- Autonomous/Driverless Integration: Modifying a commercial rack to accept an autonomous steering motor often results in space-inefficient or a significant increase in mass. A custom architecture was deemed strictly necessary to cleanly and robustly integrate the Steer-by-Wire (SBW) actuator required for the Formula SAE Driverless events.

Figure 19: UT26 steering rack internals

2.3.1. SBW

The Formula SAE Driverless competitions require an autonomous actuation system capable of steering the vehicle without driver input. This system is designated as the Steer-By-Wire (SBW) system. Because the UT26 steering rack was a custom in-house design, the housing and internal gearing were tailored specifically to accommodate this hardware seamlessly.

For the UT26 system, the SBW integration was implemented as a direct-drive configuration. Rather than utilizing external belts or secondary gearboxes that introduce compliance and friction, the autonomous steering motor is coupled directly into the pinion gear using a D-shaft motor collar, paired with a D-slot in the custom pinion gear. In all, this system achieves a 27.3% mass down from UT25.

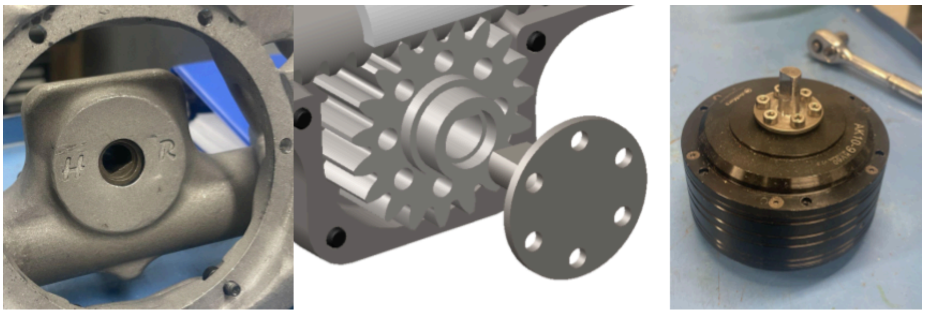

Figure 20: D-shaft motor collar used for direct drive to pinion gear.

This direct-drive architecture significantly minimizes mechanical backlash and reduces rotational inertia. Consequently, it provides the autonomous system with precise, high-fidelity control over the steering rack's linear position, ensuring rapid and accurate slip-angle adjustments during Driverless dynamic events.

To support this system, a steering motor/rack mount manufactured using additive metallurgy was utilized. This generatively designed structure was made in Fusion 360, using loads taken from the Suspension team's tube calculations (tie rod forces), driver loads on the steering column, and the DV motor's torque outputs.

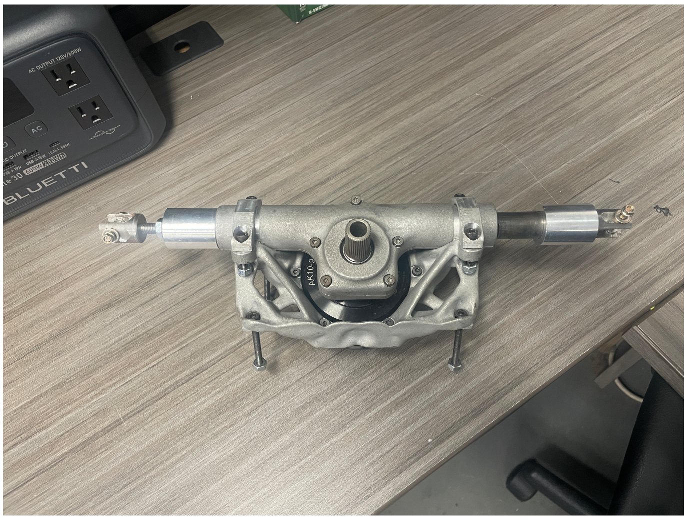

Figure 21: The SBW assembly off of the car.

In addition with simulation loads from the Vehicle Dynamics team, the piece was repeatedly optimized for mass and stiffness, then evaluated in Ansys using FEA, to ensure it does not reach 100MPa of von Mises stress under load, a value determined from testing a material sample for fatigue failure with the Engineering Materials Research group, in addition to a email conversation between Mo Taban (UT26 lead) and Bharat Mehta. An excerpt is given below for reference.

> " For components such as bellcranks; I don't think they get a lot of high load situations (probably cornering+braking) but usually need to design for low load. With fatigue I would think of two things: surfaces and high cycle fatigue.
>
> Surfaces in metals are extremely important to consider when designing for fatigue strength since that is where a killer crack could form. Check the bell crank that broke and see if you can find a defect (1 mm size or so) at part

surface where it broke. I would highly recommend sand blasting in full part as a rule of thumb; and machining the surfaces where the part mates with other components. That is easy to get by undersizing the hole by 2 mm and then drill it out to exact size. I recommended holes of 3 mm for M5/M6 holes to make sure everything fits. AM components also have residual stress when you build it, so sometimes holes far away could be inexact as compared to initial CAD component. To get rid of this stress, you heat treat the part and then do machining as per CAD.

High cycle fatigue: we assumed a lower value both for yield (structural design) and fatigue as you then include a factor of safety to your design factor of safety in CAD; so it helps to prevent failures. This factor of safety then accounts for two things: a shortcoming in CAD designer not aware 100% of design loads in dynamic cases AND stochastic defects in AM components which can be few large porosities in your component. Both these factors were the reason I always recommended 100 MPa for fatigue and taking the lower yield strength in datasheet for structural parts. We also did post treatment called hot isostatic pressing (HIP) for suspension components. There is a company Quintus, Sweden who were a research partner for me and they did this HIP for all suspension components and we saw benefits in static loads before failure (I think by 25%). What this process does is that it closes the pores and makes the microstructure more consistent so you can achieve better static and fatigue strengths in metallic printed components.

We have been printing uprights, printed motor jackets in CFS for the last 4 years; I was really happy when we first managed it. It took everyone (including me) a lot of hours to get it done. Fortunately I have never heard anything breaking, so I believe that is due to the safety factors and awareness of design for AM.

Good luck with your ambitions!

Regards, Bharat "

The specific loads for designing this mount were taken from multiple sources
- Tie rod forces from the Suspension Team (Sprenger Special SS)
- Steering Column Push forces from the mentioned report from Section 2.2.2
- DV Motor stall torques from the general Driverless Team
- Bump steer situations from a specific testing course from the Vehicle Dynamics Team data

It should also be noted that while this system did provide mass savings as well as simplicity in components, assembly of this SBW build along with the steering column on the car was incredibly tedious. An unrelated tab beneath the DV motor prevents the removal of the motor without also removing the entire mount/ steering rack. Future systems should be prototyped with accurate proportions to ensure assembly fluidity.

Another frustration that emerged during design is the low location of the DV motor. Rule F.5.14 dictates that "Steering system racks or mounting components that are external (vertically above or below) to the Primary Structure must be protected from frontal impact."

Should the component be external, a protective structure according to the following requirements must be constructed.

- It must be constructed of closed-section steel tubing matching "Size C" (25mm x 1.2mm minimum) or an approved structural equivalent (Rules F.5.14.a and F.3.2.1.n).
- It must extend to the vertical limit of the steering component(s) (Rule F.5.14.b).
- It must extend to the local width of the chassis (Rule F.5.14.c). It must meet standard monocoque attachment strengths if it is not welded directly to a tube frame (Rule F.5.14.d)

This results in the delicate balance of raising the motor location to prevent the creation of new protective structures, and keeping it low to optimize according to the Vehicle Dynamics team's objectives.